

Identification of Candidate Alkylator-Induced Cancer Susceptibility Genes by Whole Genome Scanning in Mice

Timothy S. Fenske,¹ Christine McMahon,⁵ Deepa Edwin,¹ Joseph C. Jarvis,² James M. Cheverud,² Matthew Minn,¹ Vikram Mathews,¹ Molly A. Bogue,⁴ Michael A. Province,³ Howard L. McLeod,¹ and Timothy A. Graubert¹

Departments of ¹Internal Medicine, ²Anatomy and Neurobiology, and ³Biostatistics, Washington University School of Medicine, St. Louis, Missouri; ⁴The Jackson Laboratory, Bar Harbor, Maine; and ⁵Department of Pathology, Division of Molecular Diagnostics, University of Pittsburgh, Pittsburgh, Pennsylvania

Abstract

Secondary malignancies are a serious adverse consequence of alkylator chemotherapy. The risk of developing an alkylator-associated malignancy is influenced by genetic background, although the relevant genetic factors are poorly understood. To screen for novel susceptibility factors, we established a mouse model of alkylator-induced malignancy. We exposed mice from 20 inbred strains to the prototypical alkylating agent, *N*-nitroso-*N*-ethylurea (ENU). ENU was a potent carcinogen in many of the strains tested, inducing 140 tumors in 240 ENU-treated mice (66% incidence of at least one tumor in evaluable mice), compared with a background incidence of 8% spontaneous tumors in 240 strain-, age-, and sex-matched control mice (relative risk, 8.4; $P < 0.0001$). A wide variety of tumor histologies were noted, including epithelial carcinomas, soft tissue sarcomas, and hematopoietic tumors. Cancer susceptibility was a heritable trait for the most common tumor types, lung adenocarcinoma ($H^2 = 0.25$), T cell lymphoma ($H^2 = 0.19$), and myeloid malignancies ($H^2 = 0.10$). Quantitative trait locus mapping identified regions on chromosomes 3, 6, 9, and 15 containing candidate genes associated with lung adenoma, lung carcinoma, and lymphoma susceptibility. This novel mouse model recapitulates many features of human alkylator-associated cancer and supports the hypothesis that susceptibility to this syndrome is influenced by inherited polymorphisms that could be used to make informed clinical treatment decisions. (Cancer Res 2006; 66(10): 5029-38)

Introduction

Secondary cancers are a major problem complicating therapy for highly curable malignancies such as breast cancer, Hodgkin's disease, non-Hodgkin's lymphoma, and childhood acute lymphoblastic leukemia (1-3). Hematologic malignancies, particularly acute myeloid leukemia, are the most common class of secondary cancers, but solid tumors such as lung carcinoma also occur at an increased frequency following chemoradiotherapy (4). The prevalence of secondary leukemias is rising for reasons which may

include improved patient survival after treatment of the primary tumor and more frequent and dose-intensive use of chemoradiotherapy. Alkylating agents cause a distinct clinical syndrome of treatment-related acute myeloid leukemia (t-AML). Alkylator-associated t-AML has a relatively long latency (5-7 years), frequently evolves from a myelodysplastic (MDS) phase, and is often associated with deletions on the long arm of chromosome 7 and/or chromosome 5 (5). Secondary leukemias have a dismal prognosis and are, therefore, a prime target for prevention and control strategies.

The incidence of secondary malignancies varies widely among studies from 1% to 25%, implying that susceptibility is likely multifactorial. Nongenetic risk factors include patient age, endocrine and metabolic status, primary tumor type, and chemotherapy dose. Inherited t-MDS/AML susceptibility factors include rare familial cancer predisposition syndromes associated with germline mutations in *TP53*, *XPD*, or *NFI* (6-8). Mice heterozygous for a null *Nfi* allele are predisposed to alkylator-induced myeloid malignancies (9), providing strong evidence that *NFI* is a susceptibility gene for t-MDS/AML. These mutant alleles may increase the risk of t-MDS/AML in affected individuals, but accounts for disproportionately few cases. More prevalent polymorphisms in these and other genes (each with modest effect) may account for more of the cumulative risk in the general population. Retrospective case-control studies have yielded conflicting findings on the association between t-AML and polymorphisms in cytochrome p450 family members. Increased risk of t-AML was associated with the common allele in the 5'-promoter of *CYP3A4* (odds ratio, 0.07 with variant allele) and lower magnitude risks (odds ratios, 2.7-2.8) were associated with poor metabolizer genotypes of *CYP2C19* and *CYP2D6* (10, 11). These findings were not reproduced in other studies (12, 13). An inactive allele of the detoxifying enzyme NAD(P)H:quinone oxidoreductase (NQO1) was found at higher frequencies in t-AML cases (12), but no association was found in other studies (13, 14). Studies examining variation in conjugating enzymes involved in phase II metabolism have shown mostly null associations. A recent meta-analysis of all published studies of glutathione *S*-transferase polymorphisms emphasized the modest and variable effect of *GSTM1* (odds ratios, 1.05-1.37), *GSTP1* (odds ratio, 1.63), and *GSTT1* (odds ratios, 1.70-4.62) variants on risk of t-AML (15).

Mouse models are powerful tools to screen for novel genetic factors that underlie complex traits such as susceptibility to drug-induced cancer. We optimized protocols to induce, detect, and analyze tumors in mice using the prototypical alkylating agent, *N*-nitroso-*N*-ethylurea (ENU). ENU is a potent mutagen causing point mutations with a bias towards A:T transversions and A:G transitions. The most common reported ENU-induced tumors in

Note: Supplementary data for this article are available at Cancer Research Online (<http://cancerres.aacrjournals.org/>).

Requests for reprints: Timothy Graubert, Division of Oncology, Stem Cell Biology Section, Washington University School of Medicine, Campus Box 8007, 660 South Euclid Avenue, St. Louis, MO 63110. Phone: 314-747-4437; Fax: 314-362-9333; E-mail: graubert@medicine.wustl.edu.

©2006 American Association for Cancer Research.
doi:10.1158/0008-5472.CAN-05-3404

mice occur in the lung, thymus, and liver. There is some evidence that genetic variability contributes to susceptibility in these tumors (16). However, the literature on ENU-induced cancer in mice is largely anecdotal, covering a limited number of strains and cancer sites. We did a systematic screen in diverse inbred strains of mice to better define the genetic contribution to alkylator-induced cancer susceptibility.

Materials and Methods

Mutagenesis protocol. To model alkylator-induced neoplasia in mice, we used the prototypical alkylator, ENU. ENU is the most potent mutagen known for mice. At typical doses (100-400 mg/kg), ENU induces point mutations roughly once every 1,000 loci (~20-30 per mouse genome; ref. 17). The 200 mg/kg dose was chosen for this study because higher doses increase toxicity without significantly increasing the frequency of mutations per genome (18). ENU administration followed minor modifications of established protocols (19). In brief, 1 g Isopac vials (Sigma, St. Louis, MO) were reconstituted by gentle heating at a volume of 10 mL 10% ethanol. The solution was then brought to a final volume of 100 mL with phosphate citrate buffer [0.1 mol/L dibasic sodium phosphate, 0.05 mol/L sodium citrate (pH 5.0)]. Interlot variability was corrected by assaying each reconstituted vial spectrophotometrically immediately before use. We noted <20% lot-to-lot variabilities in ENU concentration. Mice were shipped into our specific pathogen-free barrier facility at 8 weeks of age from the research colony at The Jackson Laboratory (Bar Harbor, ME). Mice ($n = 240$ per cohort, equal number of each sex) received two doses of ENU (100 mg/kg, i.p.) or no treatment ($n = 240$ mice) at 9 and 10 weeks of age. Mice were observed daily for signs of illness (e.g., hunched posture, pallor, rapid breathing). All studies were conducted with the approval of the Animal Studies Committee at Washington University School of Medicine. Mice were sacrificed and analyzed when moribund or if they reached 16 months postinjection.

Hematologic analysis. Complete blood counts with automated five-part differentials were determined with a Forcyte veterinary cell counter (Oxford Sciences, Inc., Oxford, CT). For flow cytometric analysis, bone marrow cells were stained with directly conjugated antibodies to Sca1, CD117, CD34, CD11b, Gr1, B220, CD3, CD4, or CD8 (BD PharMingen, San Diego, CA). Scatter-gated events (25,000) were acquired on a FACScan (BD Biosciences) and analyzed with FlowJo software (ver 4.5.1, Treestar, Inc., Ashland, OR).

Histology. Tissues were fixed in 10% formalin and embedded in paraffin. Five-micron sections were stained with H&E. Peripheral blood, bone marrow smears, and spleen touch preps were stained with May-Grünwald/Giemsa. All slides were reviewed in a blinded fashion by a veterinary pathologist and a clinical hematopathologist.

Statistical analysis. Cumulative probability of survival was estimated by the Kaplan-Meier method. Broad-sense heritability (H^2) was estimated using an ANOVA model with strain as a random factor and cancer phenotype (absent, present) as the dependent variable (20). The variance in cancer incidence between strains is the total genetic variance, whereas the variance within strains is environmental in origin (21). Broad-sense heritability is the ratio between strain variance to the total phenotypic variance (between-strain variance + within-strain variance). Genetic correlations among cancers were calculated using MANOVA, with strain as the factor and the five cancer phenotypes (lung adenoma, lung adenocarcinoma, lymphoma, myeloid leukemia, and gastrointestinal carcinoma) as the dependent variables. Environmental correlations among cancers are given by the residual correlation matrix from the MANOVA.

Quantitative trait locus mapping. The genotypes of 13,287 single nucleotide polymorphisms (SNP) were obtained for the 20 strains in this study from the Wellcome-CTC Mouse Strain SNP Genotype Set (<http://www.well.ox.ac.uk/mouse/INBREDS>). This set of markers places an informative SNP approximately every 160 kb across the genome. In a modification of published *in silico* mapping techniques (22), a nested ANOVA model was used to test for differences in cancer frequency between genotypes at each SNP. The use of dichotomous-dependent variables

(cancer absent/present) is in formal violation of the ANOVA model because residuals are not normally distributed, but in practice, dichotomous-dependent variables can be usefully employed in linear models (23). We controlled for multiple comparisons using the false discovery rate approach (24). When a plot of $-\log_{10}(\text{rank})$ versus $-\log_{10}(P)$ deviated markedly from linearity, the null hypothesis that no quantitative trait locus (QTL) exists was rejected. QTLs were eliminated from further consideration if there was 100% concordance between strain distributions at multiple loci because of the inability to discriminate true QTLs from "shadow" QTLs in these instances (25). Candidate regions were defined by the QTL SNP and adjacent SNPs that retain significant association with the cancer phenotype ($P < 0.05$). All annotated genes within these intervals were identified using build 35 of the mouse genome.

Results

Hematologic variables vary among inbred mouse strains.

We selected 20 inbred strains designated highest priority by the Mouse Phenome Project steering committee (The Jackson Laboratory). These strains were chosen to represent the diversity of inbred mouse strains and include the most commonly used strains. Although some strains in this set are relatively closely related to one another (e.g., SJL/J, SWR/J, and FVB/NJ; C57L/J, C58/J, and C57BL/6J), analyses of the relationship between similarities in cancer experience and genotype indicates no significant similarity in cancer susceptibility among related strains. Therefore, these strains can be considered as independent with respect to cancer susceptibilities. We first asked whether hematologic variables differed among these strains at baseline. Age- and sex-matched mice ($n = 24$ per strain) were obtained from The Jackson Laboratory research colony. Baseline hematology studies were done at 9 weeks of age. All variables have significant ($P < 0.0001$) heritable components (Supplementary Table S1). Hematologic variables are not genetically correlated with each other. There are significant sex differences for each of the hematologic variables with males having higher values on all variables, except lymphocyte count for which females have the higher level. There are also significant sex by strain interactions, indicating genetic variation in levels of sexual dimorphism for WBC count, hemoglobin, hematocrit, and platelet count. For these traits, some strains are sexually dimorphic, whereas others are monomorphic. Heritability values for the hematologic variables were also obtained separately by sex. All traits are significantly heritable in both sexes ($P < 0.0001$), with heritability values ranging from a low of 15% for hematocrit in males to a high of 56% for lymphocyte count in males.

We compared the WBC values obtained in this study to previously reported values for the same strains (26). Overall, there is no significant difference in WBC values between the studies. However, the rank orders of the strain-specific values did vary from study to study. The correlation between strain means, or repeatability, across the two studies is 0.61 in females and 0.56 in males. These are only moderate repeatabilities and show that the different environments and procedures followed in the two studies interact with the strains' genetic backgrounds to modify these phenotypes.

Mice are highly susceptible to alkylator-induced cancer.

ENU injections were well-tolerated in all strains. Necropsy data were adequate to characterize tumors in 172 ENU-treated and 191 control mice. The most common tumors were hematopoietic, with the lymphoid lineage affected more often than the myeloid lineage (Table 1). Benign and malignant lung tumors were frequently

Table 1. Spectrum of tumors induced by ENU in a survey of 20 inbred strains

Tissue	Histology	ENU	Control
Hematopoietic	Lymphoma	42	6
	Myeloid leukemia	9	1
	Myelodysplasia	4	1
	Histiocytic sarcoma	1	3
Lung	Adenoma	13	2
	Adenocarcinoma	30	1
Gastrointestinal	Adenoma, carcinoma	9	0
Genitourinary	Adenoma, carcinoma	12	0
Breast	Carcinoma	1	1
Liver	Adenoma	7	0
	Hemangioma	3	0
Skin	Carcinoma	3	0
	Fibroma	1	0
Other	Sarcoma	10	3
Total tumors		145	18
Evaluable mice		172	191
Mice with ≥ 1 tumor		114	15
Cancer incidence		0.66	0.08

NOTE: Twenty-four mice from each of 20 strains were divided equally into ENU and control groups. The total number of tumors identified in each cohort (and mice bearing at least one tumor / evaluable mice) is shown.

observed. A variety of other tumors of epithelial origin were noted in the gastrointestinal tract (e.g., stomach, large intestine, rectum) and genitourinary system (e.g., uterus, ovary, kidney). Less common ENU-induced tumors included fibrosarcoma (two cases), schwannoma (one), rhabdomyosarcoma (one), pheochromocytoma (one), breast carcinoma (one), and hemangiosarcoma (one). Overall, ENU-treated mice had a significantly increased risk of developing at least one tumor (relative risk, 8.44; 95% confidence interval, 5.13-13.88; $P < 0.0001$ by Fisher's exact test). Multiple independent tumors were identified in some mice ($n = 30$ with two tumors, $n = 6$ with more than two tumors).

Susceptibility to lung and hematopoietic tumors varies by strain. A wide variation in susceptibility between strains was observed for the three most commonly encountered ENU-induced malignancies (lung carcinoma, lymphoma, and myeloid malignancies). Lung carcinoma occurred in 50% or more of the A/J, PERA/Eij, and SWR/J mice treated with ENU (Fig. 1A). Lymphoma developed at a rate of 50% or more in AKR/J, C58/J, C57BL/6J, and NOD/LtJ mice (Fig. 1B). Myeloid malignancies (defined here as acute myeloid leukemia, granulocytic sarcoma, or myelodysplasia) were observed in four out of five (80%) evaluable SWR/J mice, three out of six (50%) DBA/2J mice, and three out of nine (33%) BALB/cByJ mice (Fig. 1C). For each of the top three cancer phenotypes, we identified at least five completely resistant strains.

ENU-treated animals from many of the strains included in this screen were incidentally found to have small lung adenomas at the time of sacrifice. They have a nonpapillary architecture and

are composed predominantly of Clara cells with occasional scattered type II pneumocytes (Fig. 2A and B). In contrast, the ENU-induced lung adenocarcinomas were highly aggressive, symptomatic tumors. Affected mice typically developed large bilateral pulmonary masses which caused rapid, shallow breathing and lethargy. Histologic examination of these tumors revealed typical features of adenocarcinoma with acinar architecture, nuclear atypia, and a propensity to invade neighboring structures (Fig. 2C and D). These tumors developed with a relative long latency of ~ 40 weeks after ENU exposure (50 weeks of age; Fig. 3A).

The lymphoid neoplasms observed were also highly aggressive. In most cases, there was symptomatic mediastinal involvement. Enlargement of mesenteric, cervical, or axillary lymph nodes was less commonly noted. Numerous abnormal lymphocytes, including frequent mitotic cells, could be found in peripheral blood smears from these mice (Fig. 2E). Bone marrow and spleen were often extensively involved, so that the megakaryocytes, maturing myeloid elements and erythroid precursors normally present in these hematopoietic tissues were diminished and partly replaced by a lymphoid infiltrate (Fig. 2F and G). In severely affected animals, nonlymphoid organs such as the liver and kidneys were diffusely infiltrated by tumor cells (Fig. 2H). Flow cytometric analysis showed an immature CD4+CD8+ immunophenotype in most cases ($n = 22$), but single positive CD4+CD8- ($n = 4$) or CD8+CD4- ($n = 11$) T cell lymphomas and B cell lymphomas ($n = 4$) were also seen (Supplementary Fig. S1). The lymphomas had a relatively short latency of ~ 20 weeks (Fig. 3B).

The myeloid malignancies were variable in presentation. Many of the animals with acute myeloid leukemia seemed lethargic or tachypneic. Laboratory studies revealed one or more of the following: leukocytosis (20-130,000 cells/ μ L), anemia (hemoglobin, 1.2-13.1 g/dL), or thrombocytopenia. Peripheral blood and/or bone marrow evaluation revealed excess myeloblasts (Fig. 2I and J); however, there were cases in which the disease was primarily extramedullary (lymph node, mediastinum, or granulocytic sarcoma). Affected mice had splenomegaly, often massive (>20 -fold enlargement) with infiltration of the red pulp by myeloblasts that encroach on or replace the megakaryocytes and erythropoietic elements normally present in the mouse spleen (Fig. 2K). In some cases, the portal triads and the sinuses of the liver were infiltrated by blasts and abnormal extramedullary hematopoiesis could be seen within the liver parenchyma (Fig. 2L). By flow cytometry, cells were positive for CD117 or CD34 and lacked expression of lymphoid markers (Supplementary Fig. S1). A minority of cases were biphenotypic (usually CD117+, CD34+, and CD3^{lo} or CD4^{lo}). Myelodysplasia was usually identified incidentally postmortem in animals which appeared to be grossly normal. These animals had mild to moderate anemia with splenomegaly and no evidence of AML or lymphoma. Histopathologic examination of the spleen revealed extensive extramedullary hematopoiesis with numerous micromegakaryocytes and dysplasia in the myeloid and erythroid lineages. Flow cytometric analysis in these MDS cases typically showed a modest increase in Ter119+ erythroid precursors in the spleen, but was otherwise unremarkable. The myeloid malignancies had an intermediate latency of ~ 30 weeks (Fig. 3C).

Given the relatively high incidence of both lymphoid and myeloid malignancies seen in AKR/J mice, a second independent cohort ($n = 40$ ENU-treated and 6 control mice) was studied. Among 37 evaluable ENU-treated mice, a similar frequency of

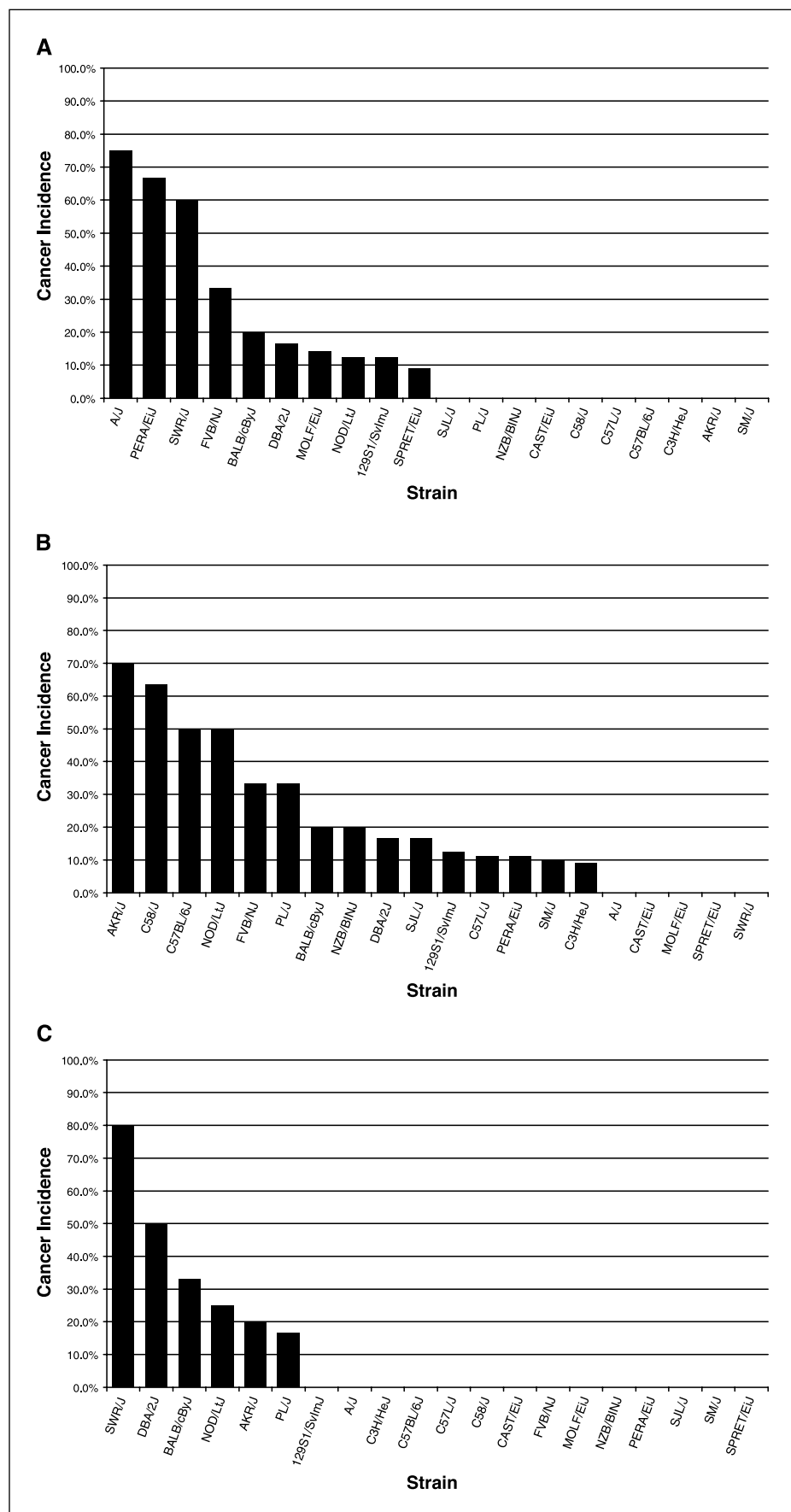


Figure 1. Incidence of three major cancer phenotypes varies by strain. The incidence of ENU-induced (A) lung carcinoma, (B) lymphoma, and (C) myeloid malignancy (acute myeloid leukemia, granulocytic sarcoma, or myelodysplasia) is shown for 20 strains of mice. The denominator is the number of evaluable mice in each strain ($n = 6-12$).

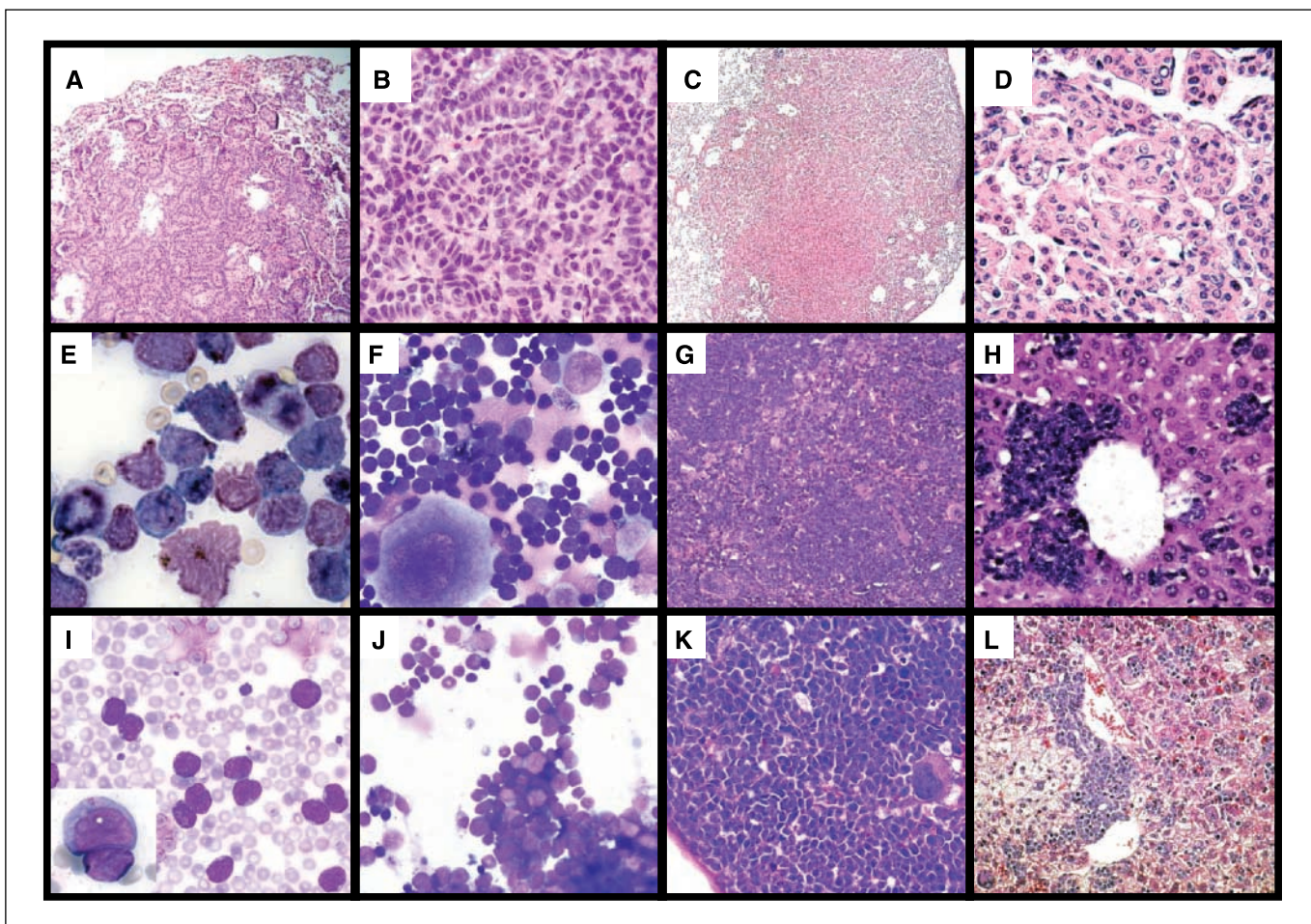


Figure 2. Histology of ENU-induced mouse tumors. *A* and *B*, pulmonary alveolar/bronchiolar adenoma. *C* and *D*, pulmonary alveolar/bronchiolar carcinoma, acinar type. *E-H*, T cell lymphoma. *I-L*, acute myeloid leukemia. *A*, hyperplasia of alveolar cells exhibiting a lepidic growth pattern (original magnification, $\times 100$). *B*, densely packed cuboidal to columnar cells with bright eosinophilic cytoplasm, predominantly Clara cells with rare type II pneumocytes interspersed (original magnification, $\times 400$). *C*, discrete tumor mass invading an adjacent bronchiole (original magnification, $\times 40$). *D*, well-differentiated adenocarcinoma composed of atypical polygonal cells which have retained the ability to form glandular lumina (original magnification, $\times 200$). *E*, peripheral blood smear shows marked leukocytosis involving predominantly abnormal lymphoid cells. Two malignant cells are seen undergoing mitosis (original magnification, $\times 500$). *F*, bone marrow is heavily infiltrated by lymphoid cells. Megakaryocytes are present, but rare mature myeloid forms are seen (original magnification, $\times 500$). *G*, spleen shows lymphoid cells infiltrating both the red and white pulp (original magnification, $\times 200$). *H*, malignant lymphoid infiltrate concentrated in periportal regions of the liver (original magnification, $\times 400$). *I*, peripheral blood smear shows blasts with fine chromatin, irregular nuclear contours, and a modest amount of cytoplasm containing occasional azurophilic granules. Note the presence of large platelets and the absence of mature myeloid cells (original magnification, $\times 500$). *J*, bone marrow. There is a predominance of myeloblasts with rare mature ring forms (original magnification, $\times 500$). *K*, spleen. Red and white pulp are diffusely infiltrated by immature, monomorphic cells. Mitotic figures are abundant. Hematopoiesis is markedly reduced (original magnification, $\times 400$). *L*, liver. Monomorphic blasts infiltrate both the periportal space and the sinuses. In addition, there is destruction of liver parenchyma and extramedullary hematopoiesis (original magnification, $\times 200$).

lymphomas and myeloid malignancies were again observed, with consistent clinical, histologic, and flow cytometric features (Fig. 3C; data not shown).

Susceptibility to lung and hematopoietic tumors is a heritable trait. The interstrain variability in cancer susceptibility was studied to determine which of these phenotypes had a significant heritable component. Most cancers were heritable (Table 2). Lung carcinoma has the highest heritability ($H^2 = 0.25$, $P < 10^{-9}$) with strains A/J (nine), PERA/Eij (six), FVB/NJ (four), and SWR/J (three) accounting for most of the cancer cases. Lymphoma had a heritability of 19% ($P < 10^{-6}$) with AKR/J (seven), C58/J (six), FVB/NJ (six), NOD/LtJ (five), and C57BL/6J (five) accounting for most of the cancer cases. Myeloid malignancies have a heritability of only 10% ($P < 0.001$) with SWR/J (four), DBA/2J (three), AKR/J (two), NOD/LtJ (two) having multiple cases. Gastrointestinal cancers have negligible heritability

($H^2 = 0.06$, $P < 0.05$) with strains CAST/Eij (three), A/J (two), C57L/J (two), and SM/J (two) having more than one case each. Finally, lung adenomas are not significantly heritable ($H^2 = 0.03$) with strains 129S1/SvImJ (three), C3H/HeJ (2) and SM/J (two) having more than one case each.

The genetic and environmental correlations between cancers are given in Table 2. Interestingly, strains with relatively high rates of lung adenomas or gastrointestinal cancers tended not to have lymphoma or myeloid malignancies. However, there is no correlation between lung adenoma and gastrointestinal cancer rates. This negative genetic association between strains indicates either that the same genes affect both kinds of cancer producing susceptibility to lung adenoma or gastrointestinal cancers and resistance to lymphoma and myeloid malignancies or that closely linked genes have these effects separately. This lack of correlation can also be accounted for by the short latency and

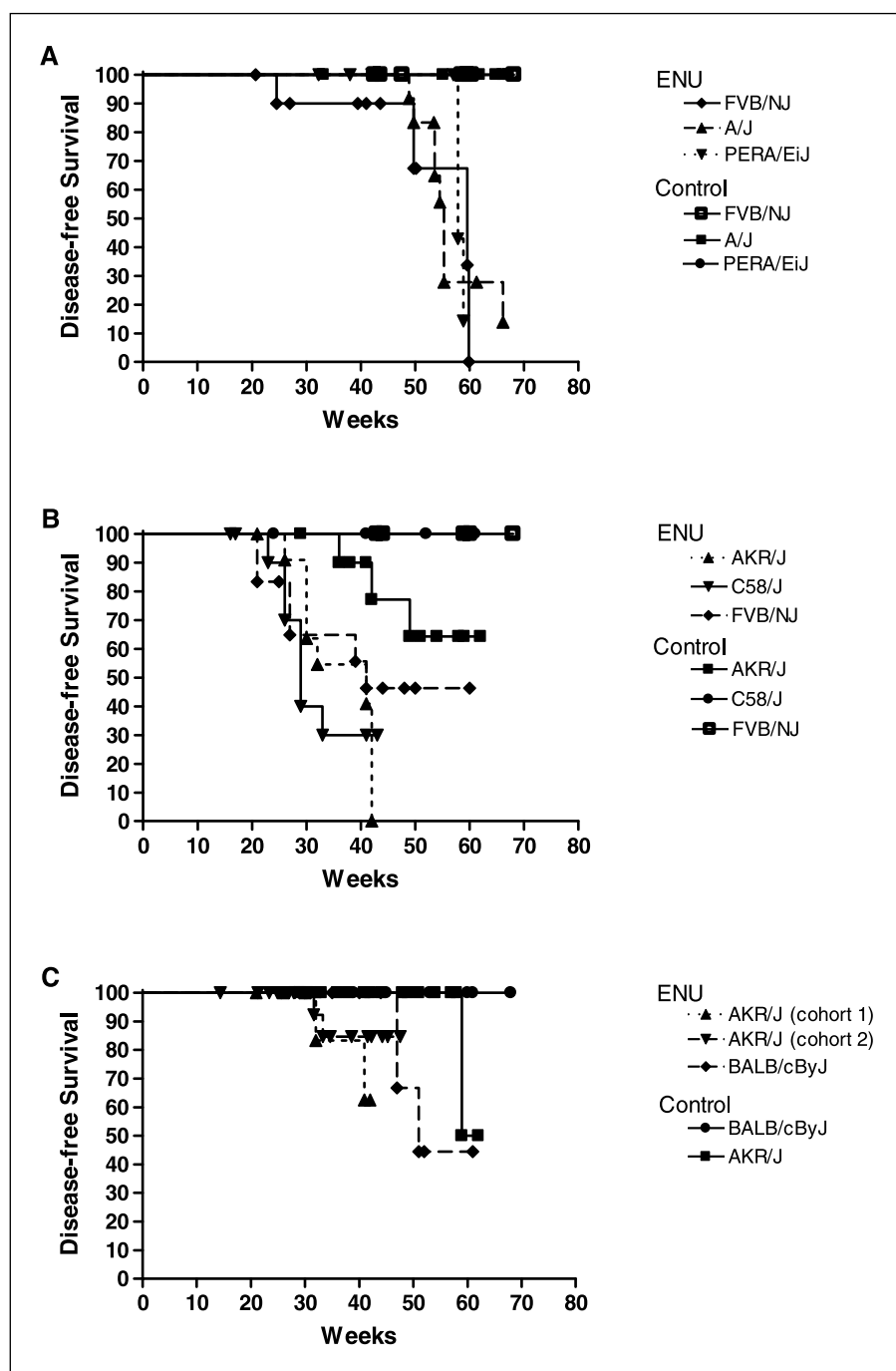


Figure 3. Survival analysis. *A*, lung carcinoma is highly penetrant with a latency of ~40 weeks after ENU exposure. *B*, lymphoma has a shorter latency (~20 weeks) and intermediate penetrance. *C*, myeloid malignancies have a longer latency (~30 weeks) and lower penetrance compared with lymphoma. Two independent cohorts of ENU-treated AKR/J mice ($n = 12$ and $n = 40$) had similar outcomes. The cumulative probability of survival was computed by the Kaplan-Meier method for each of the three end points with all other outcomes censored. Strains selected for this analysis had the highest incidence of the cancer phenotype and fewer than half of the observations censored.

high mortality of the hematopoietic tumors obscuring susceptibility to the longer latency lung and gastrointestinal tumors. There are no significant environmental correlations between cancers (Table 2).

QTL mapping. Whole genome scans were done to identify regions associated with susceptibility to the most prevalent alkylator-induced tumors observed in these 20 strains. For each of the major tumor types, loci were found that significantly diverge from a null hypothesis of no association (Fig. 4). A false discovery threshold of 10% was used. For lung adenoma susceptibility, four loci were identified on chromosomes 3, 6, and 9. Thirty-four annotated genes are contained within these four QTLs (Table 3),

including several encoding cell surface proteins (*Cd276*, *Cd1d1*, and *Sdfr1*) and transcription factors (*Pml* and *Pax4*). Lung adenocarcinoma susceptibility was associated with 10 potential genomic intervals. At two of these (both on chromosome 15), the clustering of sensitive and resistant strains was unique. One of these regions contains the prolactin receptor gene, *Prlr* (Table 3). The other loci had identical strain distributions, representing either multiple QTLs each with modest effects or the shadow of a single QTL cast on multiple sites with nonsyntenic associations (25). Because we cannot differentiate between these two possibilities, these potential QTLs were eliminated from further consideration. Lymphoma susceptibility mapped to two regions

on chromosomes 3 and 15, one of which contains the gene encoding Sprouty1, an antagonist of fibroblast growth factor signaling (Table 3).

Discussion

We performed a screen in mice to define the contribution of genetic variability to alkylator-induced cancer susceptibility. We mutagenized mice with ENU and did extensive phenotypic analysis on the resulting tumors. The drug, dose, and schedule of administration were well-tolerated in all 20 strains examined. ENU was a potent carcinogen, inducing a large number of tumors with significant interstrain variability. The most common cancer phenotypes were lung adenocarcinoma and hematopoietic malignancies of both the lymphoid and myeloid lineages. The heritability of these traits is similar to the heritabilities of common human phenotypes studied in partially inbred populations, such as plasma insulin levels ($H^2 = 0.32$), blood pressure ($H^2 = 0.21-0.45$), and measures of lung function ($H^2 = 0.35-0.41$; ref. 27). A large study of cancer incidence in twins found that ~40% of cancer risk was heritable (28), emphasizing the importance of genetics, environment, and gene/environment interactions in determining cancer risk. Heritability estimates in the current study are, admittedly, for very artificial populations. Nevertheless, they are an accurate measure of the variance in cancer susceptibility attributable to genetic background. The strains chosen are a standard set in mouse genetics. A range of inbred strains and *Mus* subspecies were included to increase genetic diversity. The high penetrance of specific cancer phenotypes we observed shows the value of this approach for the identification of genetic susceptibility factors for alkylator-induced cancer.

Resting blood counts varied little within strains and were concordant with previously published results (26). There was significant interstrain variability in total leukocyte count, neutrophil count, lymphocyte count, hemoglobin, hematocrit, and platelet count, demonstrating that the size of these hematopoietic compartments is under genetic control. Previous studies have mapped QTLs that affect peripheral blood leukocyte counts, lymphocyte proportions, and hematopoietic stem cell number and function (29, 30). In the present study, baseline hematologic variables were not correlated with cancer incidence after ENU treatment. These results suggest that distinct genetic pathways affect basal hematopoiesis and susceptibility to alkylator-induced hematopoietic malignancies.

We found a high rate of both premalignant and malignant lung tumors in several strains of mice following exposure to ENU. In

some strains (e.g., A/J, PERA/Eij, SWR/J), the incidence of lung cancer exceeded 50%. Several other strains (e.g., the C57-related strains C57L/J, C58/J, and C57BL/6j) were completely resistant. It has been known for many years that certain inbred mouse strains have increased susceptibility to spontaneous lung tumors, and that strains with a high (e.g., A/J, SWR/J) or intermediate (BALB/c) spontaneous rate of lung tumors are also more susceptible to chemical induction of tumors using cigarette smoke, tar, or purified chemical carcinogens, including ENU (16, 31). Our results update these earlier studies using modern strains and extend them to include several commonly used laboratory and wild-derived strains (SPRET/Eij, MOLF/Eij, and CAST/Eij) not previously evaluated for this phenotype.

A large number of pulmonary adenoma susceptibility (*Sluc*, *Pas*; refs. 32, 33) and resistance (*Par*; ref. 34) loci have been mapped, and several candidate genes have been cloned, notably *Kras2* (the murine homologue of human *KRAS*; ref. 35). *Kras2* is frequently mutated in ENU-induced pulmonary adenomas (36) and the *Kras*^{G12D} allele efficiently induces pulmonary adenomas when conditionally expressed in the lung (37). We did association mapping to identify potential cancer susceptibility loci. Several interesting candidate regions were identified, although these results need to be validated and complemented using traditional intercross mapping strategies because of the known statistical power limitations of this technique (38). We found four loci on chromosomes 6, 9, and 3 associated with lung adenoma susceptibility. One of these (on chromosome 6 at ~28 Mb) is near a susceptibility locus (*Sluc7*) previously mapped using recombinant congenic strains (30). The remaining three QTLs are not closely linked to previously described loci.

There is increasing awareness that alkylating agents increase the risk of lung adenocarcinoma in humans. This is particularly evident in patients with Hodgkin's disease where the relative risk ranges from 4.2 to 6.8, and is a function of increasing alkylator dose (4). The genetic basis of human susceptibility to lung cancer is not well-understood, but at least one candidate susceptibility locus has been mapped to chromosome 6q23 (39), a region not syntenic to the QTLs we identified in mice. Our analysis has identified two potential lung carcinoma susceptibility loci on chromosome 15. Three susceptibility loci (*Sluc 24*, *25*, and *26*) have been mapped to this chromosome previously (32). *Sluc24* is tightly linked to the interval we identified containing the prolactin receptor gene. *Sluc25* is close to the distal QTL we identified on chromosome 15 at ~38 Mb.

We found a high frequency of aggressive ENU-induced T cell lymphomas in several strains, with AKR/J and C58/J showing the

Table 2. Heritability and correlation of cancer phenotypes

	Lung adenoma	Lung carcinoma	Lymphoma	Myeloid leukemia	GI carcinoma
Lung adenoma	0.03	-0.11	-0.02	-0.02	0.04
Lung carcinoma	0.09	0.25	-0.13	0.11	0.06
Lymphoma	-0.71	-0.20	0.19	-0.16	-0.06
Myeloid leukemia	-0.85	-0.08	0.23	0.10	0.09
GI carcinoma	0.03	-0.08	-0.45	-0.61	0.06

NOTE: Broad-sense Heritability (diagonal, shaded), genetic correlations (below diagonal), and environmental (above diagonal) correlations between cancer types for a set of 20 inbred mouse strains. Values statistically significantly different from zero are in boldface.

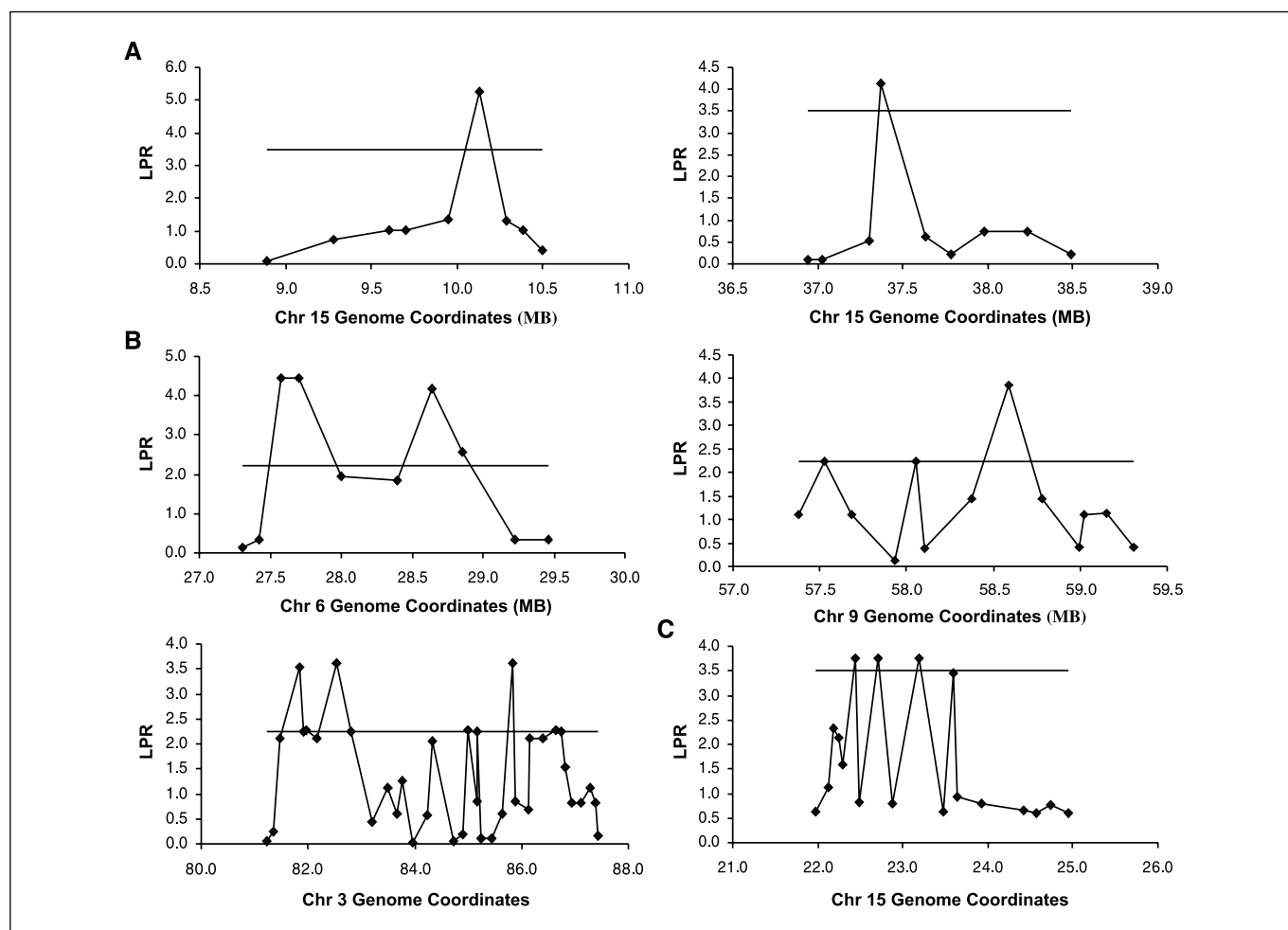


Figure 4. Genomic loci associated with susceptibility to alkylator-induced cancers. The log probability ratios (*LPR*) are shown around the genomic intervals associated with susceptibility to (A) lung carcinoma, (B) lung adenoma, and (C) lymphoma. Horizontal line, a false discovery threshold of 10%. Two QTL on chromosome 3 for adenoma susceptibility are depicted on a single plot.

highest incidence. Most strains showed intermediate susceptibility, and several strains were completely resistant (A/J, SWR/J, and the wild-derived strains). These findings are consistent with data from The Jackson Laboratory in which the frequency of spontaneous lymphomas is reported to be highest in AKR/J and C58/J, and was negligible in A/J and SWR/J (40). Lymphomas arise spontaneously in AKR/J, C58/J, and other strains by somatic recombination of latent murine leukemia viruses that activate oncogenes or inactivate tumor suppressors via insertional mutagenesis (41). Most of the recombinant inbred lines between AKR/J and DBA/2J (AKXD) are also highly susceptible to B and T cell lymphomas. The lymphomas we and others have observed in treated AKR/J and C58/J mice, therefore, represent the cumulative effect of somatic mutations induced by ENU and retroviral integration. Treatment-related lymphoid malignancies are rare in humans, but do occur (42). Therefore, mapping the susceptibility alleles for ENU-induced lymphomas may have potential for improving human health.

Several strains in our survey were susceptible to a spectrum of ENU-induced myeloid malignancies that ranged from myelodysplasia (e.g., SWR/J), to granulocytic sarcoma (e.g., DBA/2J), and acute myeloid leukemia (e.g., AKR/J, BALB/cByJ, and NOD/LtJ).

These phenotypes have not been reported in prior ENU screens. None of the commonly used modern inbred strains has a significant spontaneous rate of myeloid leukemias. In the course of generating the inbred AKR/J strain, Jacob Furth described a subline highly susceptible to myeloid leukemia which, unfortunately, was subsequently lost (43). Although most of the AKXD RI lines develop lymphomas exclusively, AKXD-23 mice develop AML with nearly full penetrance by 1 year (44). BXH-2 recombinant inbred mice also develop AML at high penetrance, whereas neither of the parental strains (C57BL/6J and C3H/HeJ) or any of the other BXH RI lines has a significant spontaneous incidence of AML (45). BXH-2 mice acquire infectious retrovirus by maternal-fetal transmission and are viremic throughout life. The identification of common retroviral integration sites in these mice has proved to be a very successful strategy for the identification of novel somatic events that contribute to AML pathogenesis (46), but again does not shed light on germline polymorphisms that affect susceptibility to drug-induced cancer. Numerous transgenic strains engineered to express fusion genes associated with human AML (e.g., AML1/ETO and PML/RARA) fail to develop AML at high penetrance, implying that AML is not a "single hit" disease. ENU mutagenesis in several of these transgenic

strains, but not in wild-type littermates, generated cooperating mutations that were sufficient to induce AML (47, 48). We observed AML in some strains after ENU, implying that inherited polymorphisms in these strains provide the first genetic "hit." This phenotype is the closest correlate to the most prevalent type of alkylator-induced cancer occurring in humans. Therefore, the strains we have identified are of particular interest for mapping susceptibility alleles for t-MDS/AML.

Although we present evidence here that susceptibility of mice to alkylator-induced cancer has a statistically significant and biologically relevant genetic component, a substantial amount of interstrain variability in this phenotype has a nonheritable cause.

This is concordant with human twin studies that show up to 60% of cancer risk has an environmental or shared genetic/environmental cause (28). These variables may include nutrition, stress, or epigenetic modification of gene expression.

In addition to the well-established link between alkylating agent exposure and t-MDS/AML in humans, it is now apparent that these drugs also increase the risk of secondary solid tumors such as lung adenocarcinoma (4), bladder carcinoma (49), and sarcoma (50). These observations provide additional validation of our ENU screen in mice and justify further study of these strains to understand the genetic basis of susceptibility to a broad range of alkylator-induced malignancies. The long-term goal of these

Table 3. QTL associated with alkylator-induced cancer susceptibility

Tumor	SNP	Log probability ratio	Interval	Candidate genes
Lung adenoma	rs13478675	4.44	6_27.423.114-6_28.851.991	<i>Grm8</i> <i>Pax4</i> <i>Fscn3</i> <i>Arf5</i> <i>Gcc1</i>
	rs13480220	3.86	9_58.102.941-9_58.995.534	<i>Stoml1</i> <i>Pml</i> <i>Islr</i> <i>Stra6</i> <i>Tbc1d21</i> <i>Cd276</i> <i>Sdfr1</i> <i>Hcn4</i> <i>Loxl1</i> <i>Neo1</i>
	rs13477230	3.62	3_81.359.882-3_82.799.868	<i>Ctso</i> <i>Tdo2</i> <i>Accn5</i> <i>Gucy1b3</i> <i>Gucy1a3</i> <i>Lrat</i> <i>Fgg</i> <i>Fga</i> <i>Fgb</i> <i>Plrg1</i> <i>Npy2r</i>
	rs13477242	3.62	3_85.631.744-3_86.825.116	<i>Sh3d19</i> <i>Rps3a</i> <i>Mab21l2</i> <i>Cd1d1</i> <i>Dcamkl2</i> <i>Hig1</i> <i>Lrba</i> <i>Cd1d2</i>
Lung carcinoma	mCV25349597	5.28	15_9.948.126-15_10.288.804	<i>Prlr</i>
	mCV24802203	4.15	15_37.305.956-15_37.631.176	<i>Ncald</i> <i>Tcfcp2l3</i>
Lymphoma	rs3671702	3.77	15_22.118.644-15_23.644.895	<i>Cdh18</i>
	rs3705939	3.68	3_36.903.931-3_37.866.074	<i>Spry1</i> <i>Spata5</i>

NOTE: SNPs defining each QTL are shown. The log probability ratio at each SNP is equal to $\log_{10}(1/P)$. The indicated interval is the genomic region flanking the QTL SNP that retains significant ($P < 0.05$) association with each cancer phenotype. Annotated genes in each interval are shown. ESTs and predicated genes were omitted.

studies is to create screening tools that will allow for prospective risk stratification of patients so that therapy can be tailored to lower the risk of secondary malignancies.

Acknowledgments

Received 9/22/2005; revised 3/1/2006; accepted 3/9/2006.

References

- Curtis RE, Boice JD, Jr, Stovall M, et al. Risk of leukemia after chemotherapy and radiation treatment for breast cancer. *N Engl J Med* 1992;326:1745–51.
- Kaldor JM, Day NE, Clarke EA, et al. Leukemia following Hodgkin's disease. *N Engl J Med* 1990;322:7–13.
- Travis LB, Curtis RE, Boice JD, Jr, Hankey BF, Fraumeni JF, Jr. Second cancers following non-Hodgkin's lymphoma. *Cancer* 1991;67:2002–9.
- Travis LB, Gospodarowicz M, Curtis RE, et al. Lung cancer following chemotherapy and radiotherapy for Hodgkin's disease. *J Natl Cancer Inst* 2002;94:182–92.
- Pedersen-Bjergaard J, Rowley JD. The balanced and the unbalanced chromosome aberrations of acute myeloid leukemia may develop in different ways and may contribute differently to malignant transformation. *Blood* 1994;83:2780–6.
- Allan JM, Smith AG, Wheatley K, et al. Genetic variation in XPD predicts treatment outcome and risk of acute myeloid leukemia following chemotherapy. *Blood* 2004;104:3872–7.
- Felix CA, Hosler MR, Provisor D, et al. The p53 gene in pediatric therapy-related leukemia and myelodysplasia. *Blood* 1996;87:4376–81.
- Maris JM, Wiersma SR, Mahgoub N, et al. Monosomy 7 myelodysplastic syndrome and other second malignant neoplasms in children with neurofibromatosis type 1. *Cancer* 1997;79:1438–46.
- Mahgoub N, Taylor BR, Le Beau MM, et al. Myeloid malignancies induced by alkylating agents in Nfl mice. *Blood* 1999;93:3617–23.
- Felix CA, Walker AH, Lange BJ, et al. Association of CYP3A4 genotype with treatment-related leukemia. *Proc Natl Acad Sci U S A* 1998;95:13176–81.
- Roddam PL, Rollinson S, Kane E, et al. Poor metabolizers at the cytochrome P450 2D6 and 2C19 loci are at increased risk of developing adult acute leukemia. *Pharmacogenetics* 2000;10:605–15.
- Naoe T, Takeyama K, Yokozawa T, et al. Analysis of genetic polymorphism in NQO1, GST-M1, GST-T1, and CYP3A4 in 469 Japanese patients with therapy-related leukemia/myelodysplastic syndrome and *de novo* acute myeloid leukemia. *Clin Cancer Res* 2000;6:4091–5.
- Blanco JG, Edick MJ, Hancock ML, et al. Genetic polymorphisms in CYP3A5, CYP3A4 and NQO1 in children who developed therapy-related myeloid malignancies. *Pharmacogenetics* 2002;12:605–11.
- Smith MT, Wang Y, Kane E, et al. Low NAD(P)H:quinone oxidoreductase 1 activity is associated with increased risk of acute leukemia in adults. *Blood* 2001;97:1422–6.
- Ye Z, Song H. Glutathione S-transferase polymorphisms (GSTM1, GSTP1 and GSTT1) and the risk of acute leukaemia: a systematic review and meta-analysis. *Eur J Cancer* 2005;41:980–9.
- Malkinson AM. The genetic basis of susceptibility to lung tumors in mice. *Toxicology* 1989;54:241–71.
- Hitotsumachi S, Carpenter DA, Russell WL. Dose-repetition increases the mutagenic effectiveness of *N*-ethyl-*N*-nitrosourea in mouse spermatogonia. *Proc Natl Acad Sci U S A* 1985;82:6619–21.
- Weber JS, Salinger A, Justice MJ. Optimal *N*-ethyl-*N*-nitrosourea (ENU) doses for inbred mouse strains. *Genesis* 2000;26:230–3.
- Justice MJ, Carpenter DA, Favor J, et al. Effects of ENU dosage on mouse strains. *Mamm Genome* 2000;11:484–8.
- Sokal RR, Rohlf FJ. *Biometry: the principles and practice of statistics in biological research*. 3rd ed. New York: W.H. Freeman; 1995.
- Falconer DS, Mackay T. *Problems on quantitative genetics*. London; New York: Longman; 1997.
- Grupe A, Germer S, Usuka J, et al. In silico mapping of complex disease-related traits in mice. *Science* 2001;292:1915–8.
- Cohen J. *Applied multiple regression/correlation analysis for the behavioral sciences*. 3rd ed. Mahwah, NJ: L. Erlbaum Associates; 2003.
- Storey JD, Tibshirani R. Statistical significance for genomewide studies. *Proc Natl Acad Sci U S A* 2003;100:9440–5.
- Cheverud JM, Ehrlich TH, Hrbek T, Kenney JP, Pletscher LS, Semenkovich CF. Quantitative trait loci for obesity- and diabetes-related traits and their dietary responses to high-fat feeding in LGXSM recombinant inbred mouse strains. *Diabetes* 2004;53:3328–36.
- Peters LL, Barker JE. Hematology, clotting, and thrombosis. Mouse Phenome Database web site. 2006;MPD:62.
- Ober C, Abney M, McPeck MS. The genetic dissection of complex traits in a founder population. *Am J Hum Genet* 2001;69:1068–79.
- Lichtenstein P, Holm NV, Verkasalo PK, et al. Environmental and heritable factors in the causation of cancer—analyses of cohorts of twins from Sweden, Denmark, and Finland. *N Engl J Med* 2000;343:78–85.
- Chen J, Harrison DE. Quantitative trait loci regulating relative lymphocyte proportions in mouse peripheral blood. *Blood* 2002;99:561–6.
- Henckaerts E, Geiger H, Langer JC, Rebollo P, Van Zant G, Snoeck HW. Genetically determined variation in the number of phenotypically defined hematopoietic progenitor and stem cells and in their response to early-acting cytokines. *Blood* 2002;99:3947–54.
- Shimkin MB, Stoner GD. Lung tumors in mice: application to carcinogenesis bioassay. *Adv Cancer Res* 1975;21:1–58.
- Tripodis N, Hart AA, Fijneman RJ, Demant P. Complexity of lung cancer modifiers: mapping of thirty genes and twenty-five interactions in half of the mouse genome. *J Natl Cancer Inst* 2001;93:1484–91.
- Gariboldi M, Manenti G, Canzian F, et al. A major susceptibility locus to murine lung carcinogenesis maps on chromosome 6. *Nat Genet* 1993;3:132–6.
- Wang M, Devereux TR, Vikis HG, et al. Pol iota is a candidate for the mouse pulmonary adenoma resistance 2 locus, a major modifier of chemically induced lung neoplasia. *Cancer Res* 2004;64:1924–31.
- Zhang Z, Futamura M, Vikis HG, et al. Positional cloning of the major quantitative trait locus underlying lung tumor susceptibility in mice. *Proc Natl Acad Sci U S A* 2003;100:12642–7.
- Malkinson AM. Molecular comparison of human and mouse pulmonary adenocarcinomas. *Exp Lung Res* 1998;24:541–55.
- Jackson EL, Willis N, Mercer K, et al. Analysis of lung tumor initiation and progression using conditional expression of oncogenic K-ras. *Genes Dev* 2001;15:3243–8.
- Darvasi A. In silico mapping of mouse quantitative trait loci. *Science* 2001;294:2423.
- Bailey-Wilson JE, Amos CI, Pinney SM, et al. A major lung cancer susceptibility locus maps to chromosome 6q23–25. *Am J Hum Genet* 2004;75:460–74.
- Naf D, Krupke DM, Sundberg JP, Eppig JT, Bult CJ. The Mouse Tumor Biology Database: a public resource for cancer genetics and pathology of the mouse. *Cancer Res* 2002;62:1235–40.
- Mucenski ML, Bedigian HG, Shull MM, Copeland NG, Jenkins NA. Comparative molecular genetic analysis of lymphomas from six inbred mouse strains. *J Virol* 1988;62:839–46.
- van Leeuwen FE, Klokmann WJ, Hagenbeek A, et al. Second cancer risk following Hodgkin's disease: a 20-year follow-up study. *J Clin Oncol* 1994;12:312–25.
- Furth J. The creation of the AKR strain, whose DNA contains the genome of a leukemia virus. *Cancer Research Institute, NIAID: Academic Press*; 1978.
- Mucenski ML, Taylor BA, Ihle JN, et al. Identification of a common ecotropic viral integration site, Evi-1, in the DNA of AKXD murine myeloid tumors. *Mol Cell Biol* 1988;8:301–8.
- Bedigian HG, Johnson DA, Jenkins NA, Copeland NG, Evans R. Spontaneous and induced leukemias of myeloid origin in recombinant inbred BXH mice. *J Virol* 1984;51:586–94.
- Li J, Shen H, Himmel KL, et al. Leukaemia disease genes: large-scale cloning and pathway predictions. *Nat Genet* 1999;23:348–53.
- Castilla LH, Garrett L, Adya N, et al. The fusion gene Cbfb-MYH11 blocks myeloid differentiation and predisposes mice to acute myelomonocytic leukaemia. *Nat Genet* 1999;23:144–6.
- Higuchi M, O'Brien D, Kumaravelu P, Lenny N, Yeoh EJ, Downing JR. Expression of a conditional AML1-ETO oncogene bypasses embryonic lethality and establishes a murine model of human t(8;21) acute myeloid leukemia. *Cancer Cell* 2002;1:63–74.
- Kaldor JM, Day NE, Kittelmann B, et al. Bladder tumours following chemotherapy and radiotherapy for ovarian cancer: a case-control study. *Int J Cancer* 1995;63:1–6.
- Hawkins MM, Wilson LM, Burton HS, et al. Radiotherapy, alkylating agents, and risk of bone cancer after childhood cancer. *J Natl Cancer Inst* 1996;88:270–8.